51p.

OBSERVATIONS ON CAVITATION DAMAGE

IN A

FLOWING SYSTEM[*]

UNPUBLISHED PRELIMINARY DATA

Frederick G. Hammitt

June 1962

OTS PRICE

XEROX $ 5.60 pl

MICROFILM $ 1.73 mf

ACKNOWLEDGEMENTS

The author would like to acknowledge the consultation and assistance of Professors R. D. Pehlke, and C. A. Siebert, of the Chemical and Metallurgical Engineering Department, and the assistance of Messrs. L. Barinka, V. Biss, P. T. Chu, V. F. Cramer, R. D. Ivany, B. Rupke, and M. J. Robinson, in the conducting of the research investigations herein reported.

Sincere thanks also are extended to the personnel of the Micrometrical Manufacturing Company for the loan of their Linear Proficorder, and assistance in its operation.

-ii-

ABSTRACT

Cavitation damage to specimens of stainless steel, carbon steel, aluminum, and plexiglas, placed in a cavitating venturi using water and mercury as test fluids is mostly in the form of irregularly shaped pits which do not change with additional exposure to the cavitating field within the limited durations utilized. The rate of damage is very high initially, decreases for a relatively short period of time, then increases again up to the maximum test durations of 150 hours with water and 270 hours with mercury. Observation of damage effects by several independent techniques, using a variety of specimen materials, with two different fluids under various fluid dynamic conditions, leads to a suggested correlating model in terms of the cavitation bubble density and energy and specimen material strength.
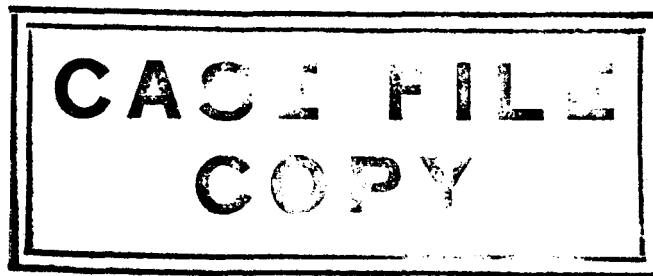
TABLE OF CONTENTS

LIST OF TABLES

LIST OF FIGURES (Continued)

I Introduction

Damage to structural materials by cavitation, perhaps assisted by ordinary erosion and corrosion, has long been a serious problem to the manufacturers and users of fluid-flow components. It has often been possible in the past to avoid the problem to some extent either by sufficiently reducing the performance-ratings of components, or by increasing system pressures. In numerous present-day applications, such as those in the aero-space field, such compromises may not be feasible, because of the over-riding necessity of minimizing sizes and weights of components. Hence, there is a strongly renewed interest in understanding the fundamentals of the cavitation damage process, so that meaningful predictions of damage to be anticipated with a variety of fluids and structural materials over a very large temperature, pressure, and velocity range can be made. While much data on various instances of cavitation damage are available in the literature, it is necessary that further systematic investigations be made under very carefully controlled and well known conditions, covering a broad range of fluid, material, and flow parameters. This paper discusses some of the results from the initial phases of such an investigation.

Because of the considerable complexities of the damage phenomenon, it is desirable that the test conditions under which damage is obtained match as closely as possible the actual operating conditions of applicable fluid components. However, this approach, if carried to an extreme, does not represent a practical ideal, because of the lack of generality

entailed, as well as the prohibitive budgetary requirements.
As the best compromise solution available, the insertion of
damage specimens into a cavitating venturi test section was
selected for the present investigation. It was felt that this
solution combined the close applicability of flow-induced
cavitation in a flowing system with a highly-simplified flow
pattern. In addition, the equipment requirement in order to
operate over a considerable range of fluid, flow, and material
parameters is relatively modest.

II Test Apparatus (1)

The test facility is a closed loop, powered by a centri-
fugal pump, and includes a plexiglas venturi test section
(Fig. 1). The venturi (Fig. 2) has a 6° included angle nozzle
and diffuser, separated by a cylindrical throat of 0.51 inches
diameter and 2.35 inches length. The two damage specimens are
inserted with their midpoint 0.79 inches downstream of the
throat exit. They consist of planar sections, located parallel
to the stream with tapered leading and trailing edges (Fig. 3,
4). They are 0.74 inches long by 0.06 inches wide, and are
submerged to a depth of about 0.20 inches into the cavitating
stream. They are located symmetrically about a vertical plane
passing through the venturi centerline, so that they are each
at the same elevation, with their axes inclined at 45° to the
vertical.

The facility has been operated with both water and mercury.
This paper is concerned mainly with the water tests, since the
mercury data are not yet fully evaluated. Throat velocities

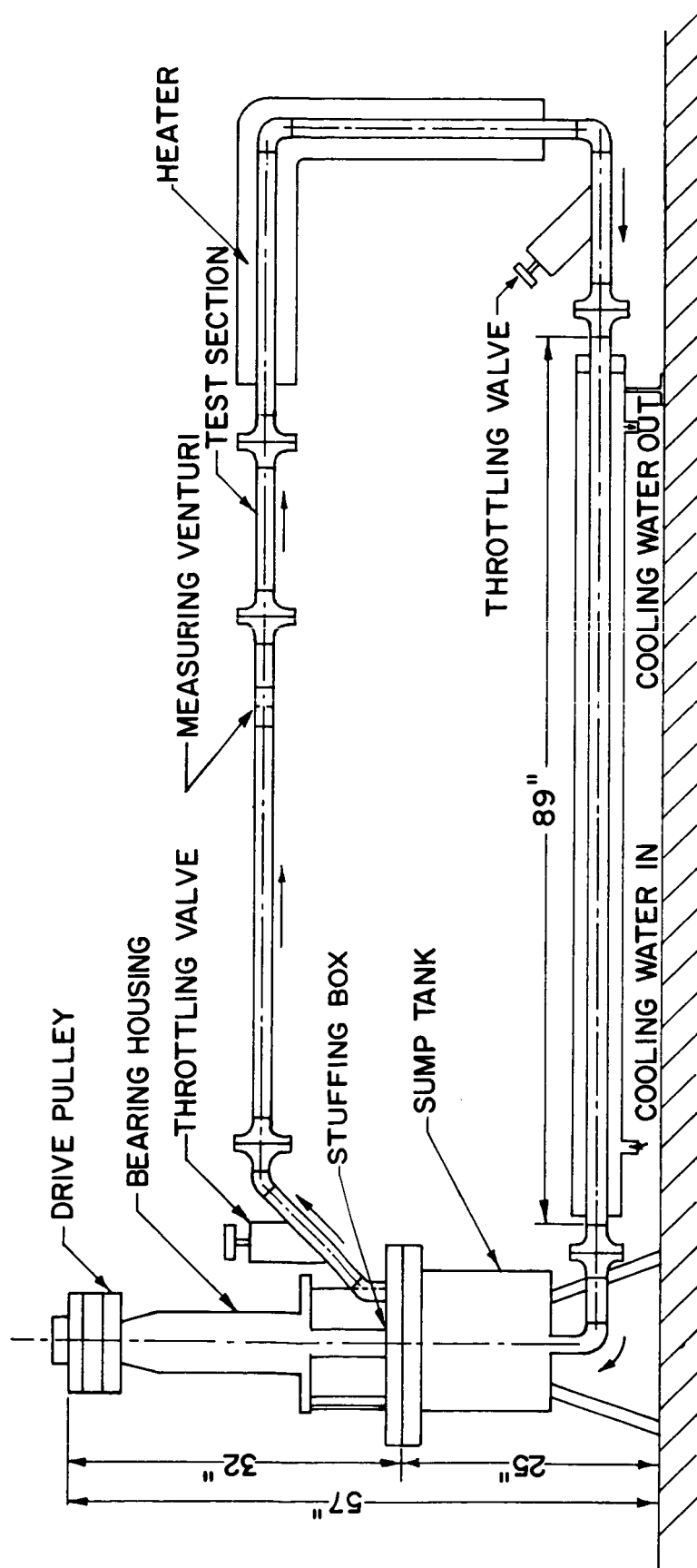Fig. 1   Overall loop layout.

-4-
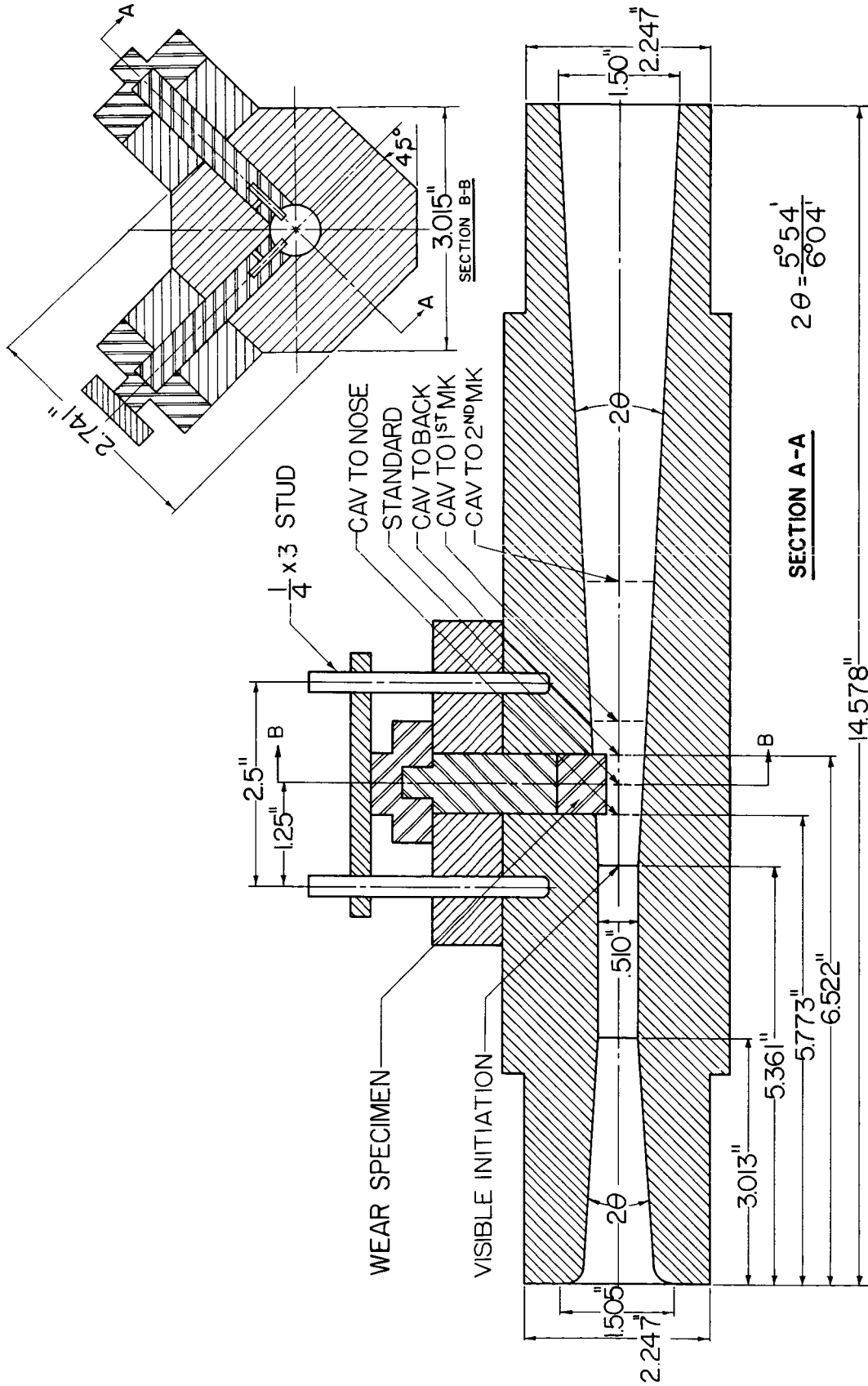
Fig. 2   Damage test venturi, showing locations of specimens and specimen holders. The dotted lines in the diffuser represent locations of cavitation termination for various degrees of cavitation. (Half-inch venturi test section No. II.)
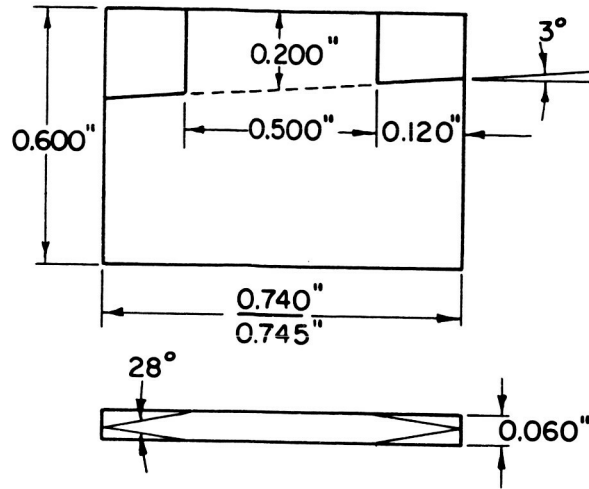
Fig. 3   Damage test specimen.
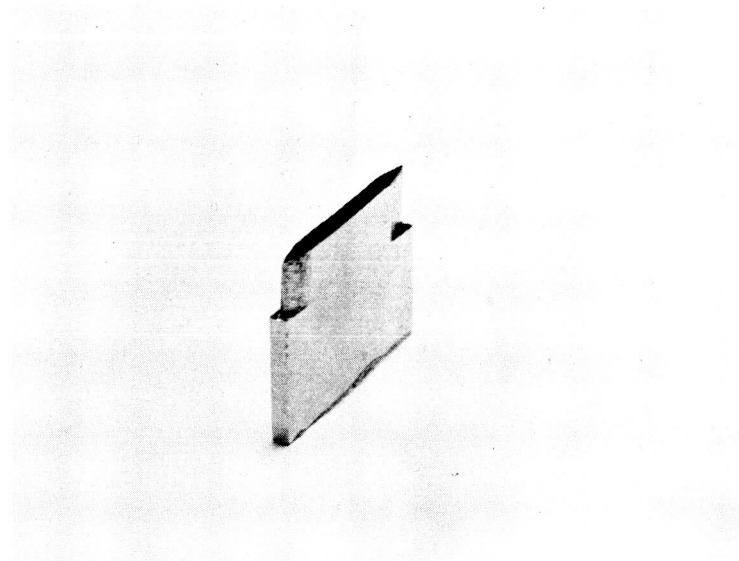
Fig. 4   Damage test specimen. The upper shadowed surface
          is the polished surface.

between about 50 and 100 ft/sec are available with water. The cavitation condition can be adjusted between "visual initiation" and "second mark" (defined in Appendix). Water temperature can be varied between about 50° F and 160° F.

With mercury, the attainable throat velocities range between about 20 and 50 ft/sec, over the same range of cavitation conditions.

Test materials so far have included carbon steel, austenitic stainless steel, aluminum, and plexiglas, in water; all but the last in mercury. In all cases, the specimens are metallographically polished prior to a test.

Further details of the facility and its operation have been given previously. (1, 2)

Operating Procedure

To the present, the maximum test duration is of the order of 100 to 200 hours. However, the specimens are removed at frequent intervals during this period for examination. These examinations always include:

 i) Tabulation of pits according to size and number

 ii) Weight measurement of specimen

 iii) Photomicrographs of unusual pit formations.

In some cases, the following items have also been included:

 i) Pit tabulation according to type and location (1)

 ii) Measurement of pit profiles using precision "proficorder[1] (1, 3)

---

[1] "Linear Proficorder" manufactured by Micrometrical Manufacturing Company, Ann Arbor, Michigan.

iii) Sectioning through a pit and observation of sub-surface
structure (1) (this destructive examination prevents
further specimen use)

iv) Irradiation of test specimens with subsequent measure-
ment of radioactive contamination in water, and
of cavitation particle size distribution using stacked,
precision filters (1, 4)

The experimental observations, to be discussed later, are
drawn from all of the above sources.

III Experimental Observations

The experimental observations of this investigation are
so far largely concerned with the early phases of cavitation
damage, i.e., relatively small individual pits, primarily,
before gross damage has occurred. Since the key to an eventual
understanding of the mechanisms producing gross damage must
lie in an understanding of these initial phases, and since
previous precise observations of the initial phases are not
numerous, it is felt that the present observations are of sub-
stantial interest.

A. Damage as Function of Time

In the present tests damage has been evaluated using two
techniques:

i) Irradiated test specimen (4)

ii) Calculation, based on pit size and number tabulation,
using a typical pit profile (1)

Direct measurement of weight loss in the water tests has not
been feasible since the loss, as a proportion of test specimen

weight, has been too small. Significant, direct weight loss measurements have been achieved in the mercury tests where the weight losses are much greater.

The absolute magnitudes of damage obtained from the irradiated specimen test (only one has so far been conducted) and from the pit volume calculations do not at present agree, although the shapes of the weight loss vs. time curves are virtually identical (Fig. 5). However, in the irradiated specimen test, there are various significant sources of error which, it is hoped, will be reduced by subsequent development of the procedure. Obviously, there are also substantial uncertainties in the pit volume calculation involving the assumption of a typical pit shape, in the extrapolation of pitting densities from a relatively small monitored surface to a larger unobserved surface, in the relation between pit volume and material volume removed,[2] etc. In the future it will be possible to obtain a direct comparison between the pit calculation results and the results of direct weight measurements in the mercury tests. However, these data are not as yet available.

Even though the absolute magnitudes of volume or weight losses are subject to uncertainty, it is believed that the consistency between tests is good, so that meaningful comparisons between the different materials, fluids, and test conditions can be drawn. This statement is based upon the reasonably

---

[2]It has so far been assumed that these are equal. However, it is known that this is not exactly true for any of the pit configurations and is probably in gross error for some (craters).
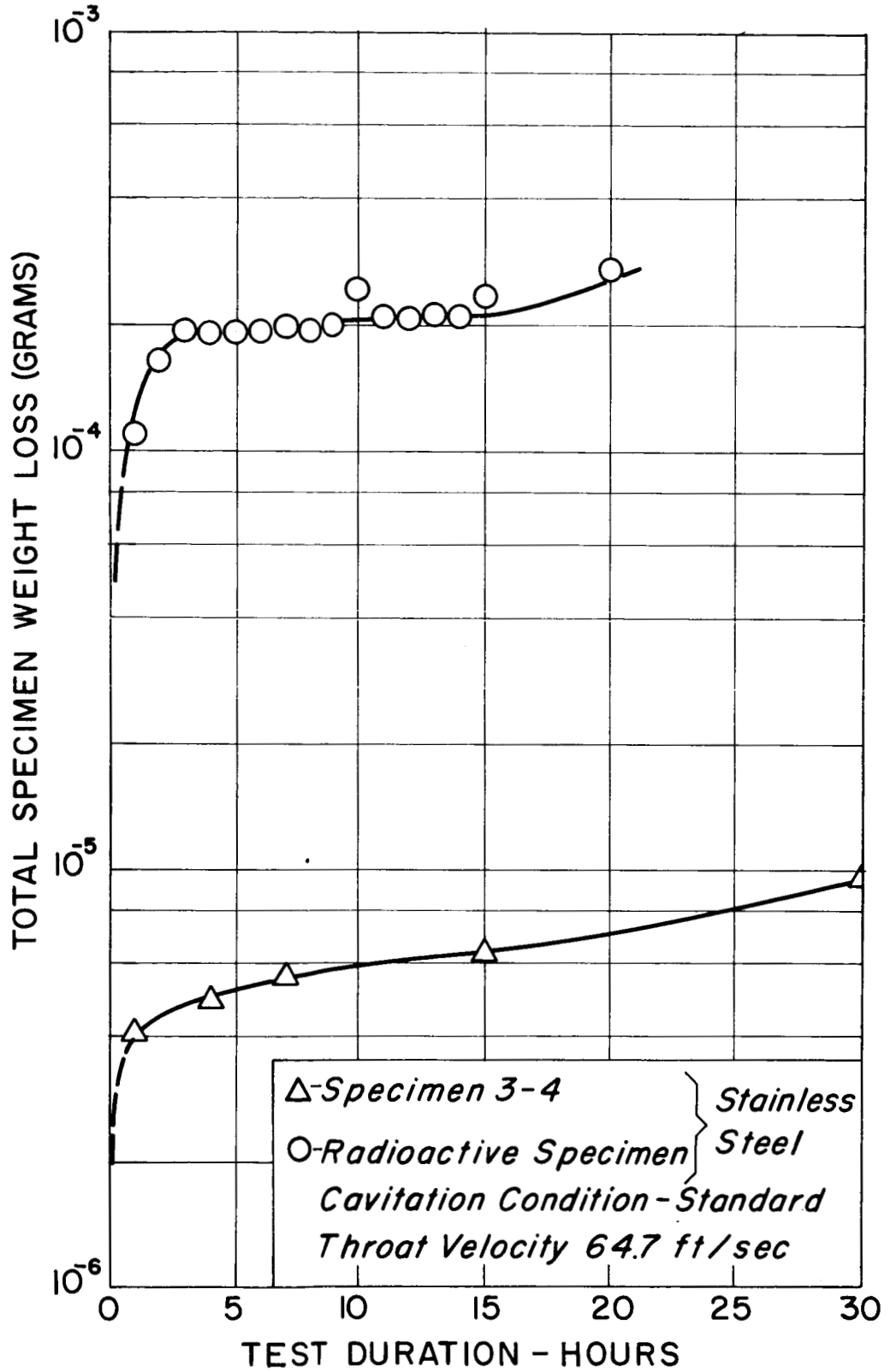
Fig. 5   Comparison of total weight loss from stainless steel
          specimens as determined by pit counting technique
          and by radioactive technique.

smooth curves obtained for volume loss as a function of time, as well as upon the virtually identical shape of the curves produced from the irradiated specimen approach and the pit calculation: two very different methods of observation.

The damage has been presented in terms of volume removed per unit area exposed, i.e., specific volume loss (cm^3/cm^2 or simply cm, representing a mean depth of penetration if the wear were uniform rather than in the form of pits). It is felt that presentation in these terms allows the most meaningful comparison possible between different materials and test arrangements.

The specific observations are discussed below.

1. Initial Rapid Damage Rate

Figures 5 and 6 show cavitation damage with water as a function of time for "standard" cavitation at 65 ft./sec. throat velocity. Damage for other cavitation conditions is also shown in Fig. 6. Although these curves are for somewhat similar conditions, their shape is typical of all the curves for either water or mercury. It is noted that there is a very rapid initial rate of damage (more apparent in Fig. 5 where greater detail is shown), showing substantial pitting after no more than one hour of exposure (first examination). After the first one to three hours, the damage rate decreases substantially, remaining relatively low for a period (up to the order of 35 to 100 hours, depending upon cavitation condition, material, etc., Fig. 6), and then climbs at an accelerated rate, at least to the maximum duration attained for water to

Fig. 6   Mean volume loss per unit area of specimen exposed
to fluid for pairs of stainless steel specimens vs.
test duration; for several cavitation conditions
with water.

date, i.e., 150 hours. However, a mercury damage curve, Fig. 7, for a maximum duration of 270 hours, shows a subsequent levelling-off and then a second accelerated climb.

It is felt that the above results are significant in three respects:

i) The absence of any "incubation period" is noted for these tests. Since the initial rapid damage rate does not result in a significant weight loss, it is felt that this initial damage may have been missed in some of the previous investigations which relied only on weight measurements for damage detection. In Fig. 5, the initial weight loss is clearly shown by the irradiated tracer test as well as by pit counts. It is noted that an apparent incubation period would result if the later, rapid damage portion of the curve (Fig. 6) were extrapolated linearly to zero.

ii) Large pits, i.e., of the same general size as the largest noted in any of the runs, are formed within the first hour or so. (Fig. 8)

iii) The wear rate generally tends to increase with time. In the present investigation, no limit to this trend has yet been found. There are, however, periods of relatively short duration during which the wear rate appears to reach a minimum.

The above effects are believed more a function of the properties of the material surface than of the cavitation condition. It is postulated that the initial rapid wear rate is a result of removal of surface defects such as inclusions or other "weak spots". Once these relatively few "weak spots" have been removed, the wear rate decreases drastically. As
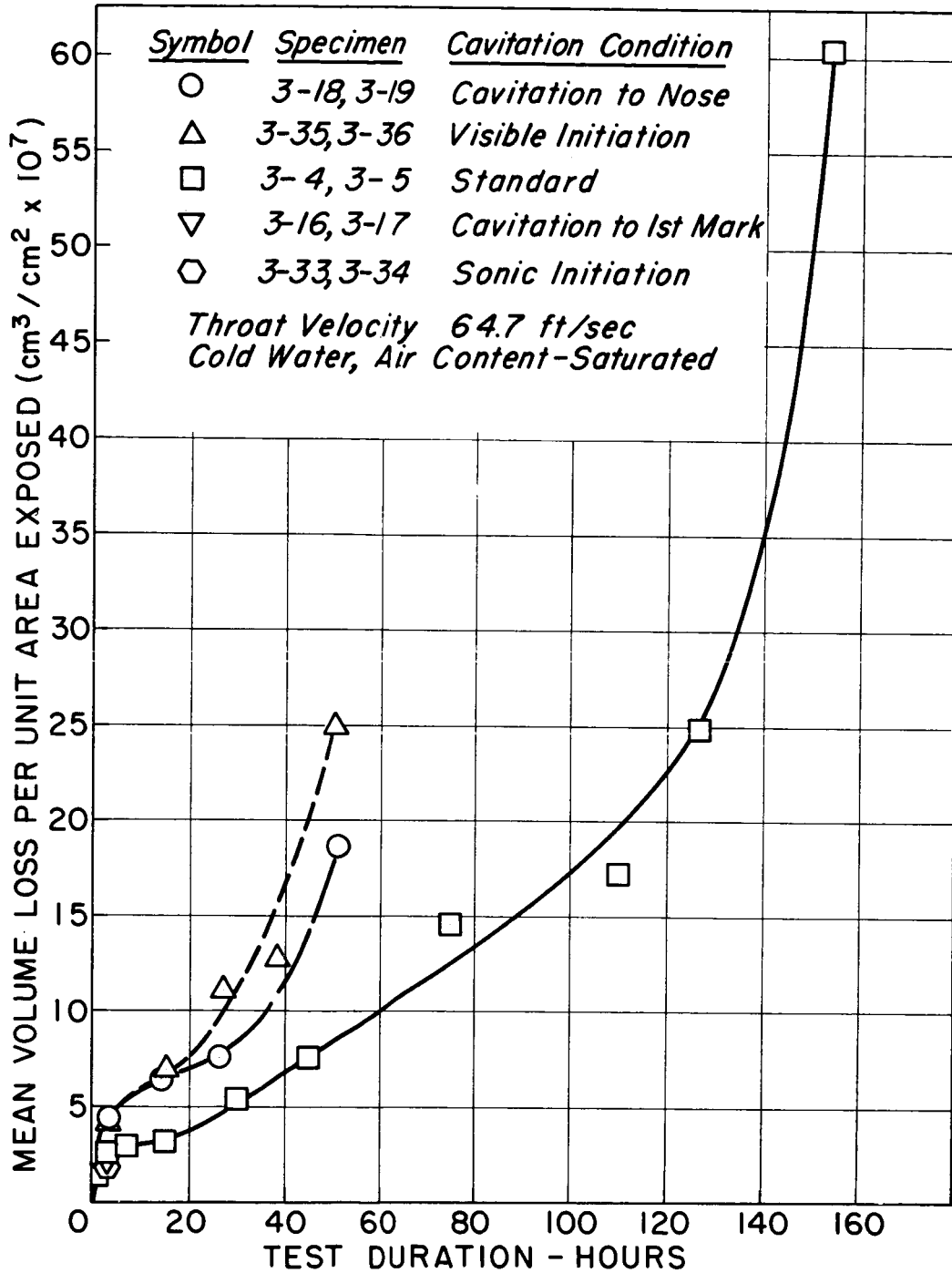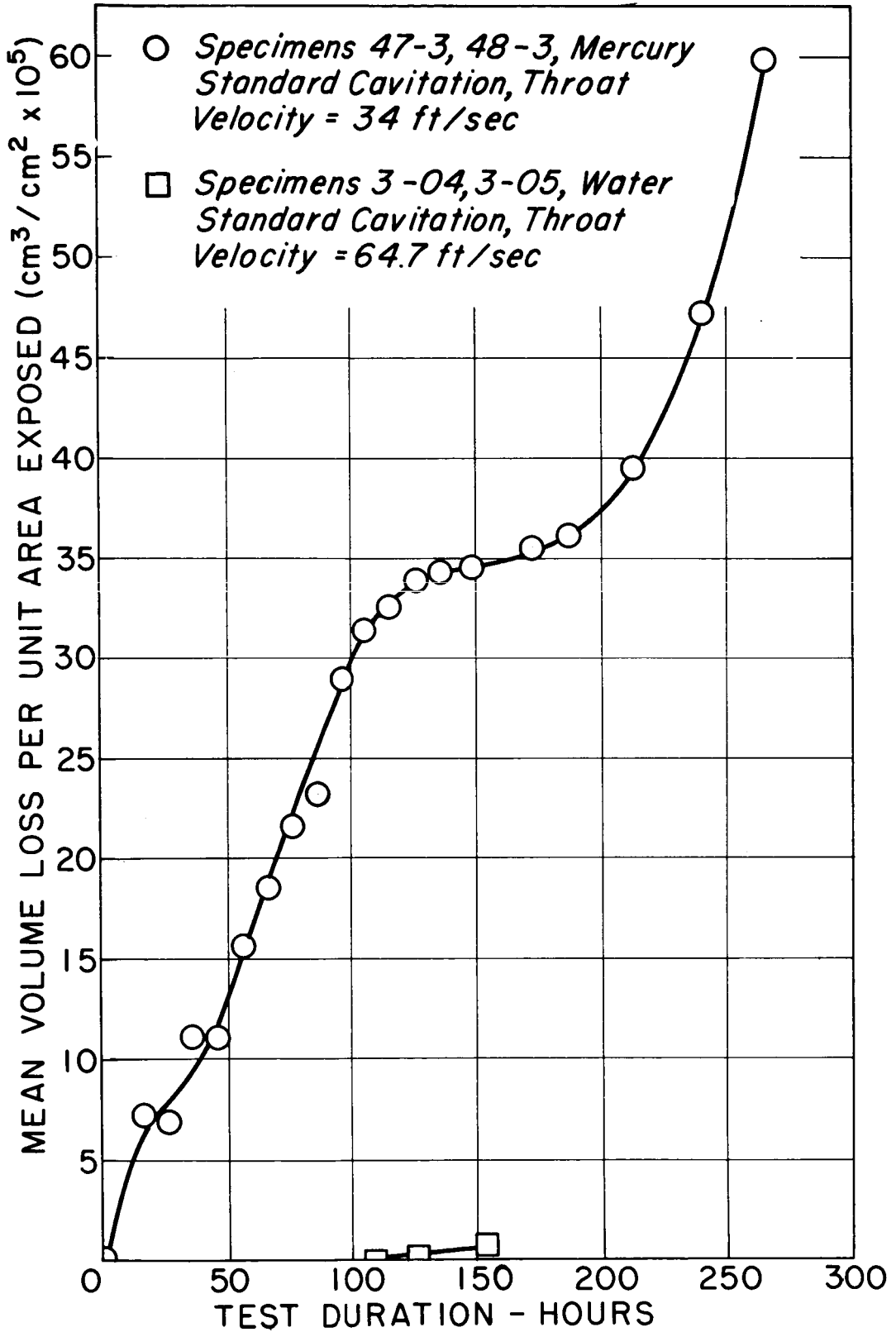
-12-

Fig. 7   Mean volume loss per unit area of specimen exposed
to fluid for pairs of stainless steel specimens vs.
test duration; for standard cavitation condition with
mercury, and comparison with water.
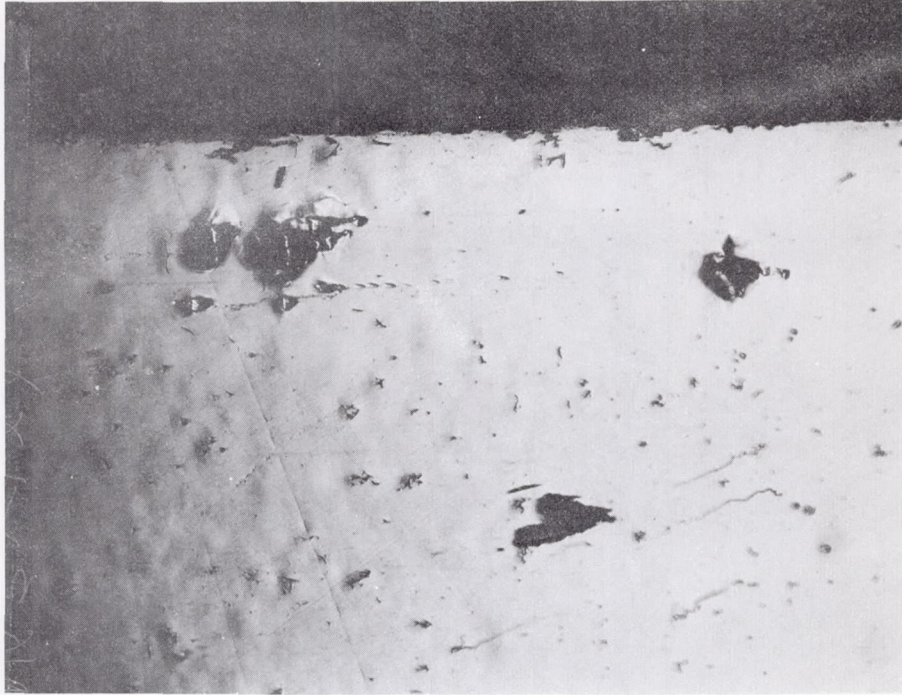
Fig. 8   Typical cavitation damage on carbon steel, for stand-
ard cavitation condition with water. (Specimen 1-19,
after 3 hours; throat velocity 64.7 ft/sec; x 100.)

the test proceeds, however, the surface tends to work-harden as the endurance limit is approached. In addition, as the amount of damage increases, there are flow perturbations due to the damage and additional area is exposed. The final shape of the damage—time curve is a result of the interplay of these various influences, and perhaps of others as yet unsuspected. In the relatively short duration tests of the present investigation, it is doubted that the feedback between surface roughening and flow perturbation is yet important.

B.　Single-Event Pitting Theory

It has been experimentally verified, within the durations of the present water tests, that the surface outline and depth of a pit, once formed, does not, in general, change during subsequent testing. This is illustrated by the photomicrographs of Figures 9 and 10, showing two particular areas, one after 15 hours of testing, and one after 30 hours, and both again after 150 hours. Intermediate duration pictures are also available,(1) as are other series taken at different locations and on different specimens. (3) These have not been included in the interest of brevity. They all illustrate the fact that while new pits may be formed in the area of an old pit, the old ones are in general not changed, at least in surface appearance. It has been demonstrated in addition, (3) that their depth profiles are also unchanged (Fig.11). Also, as previously mentioned and as illustrated by Fig. 8, typical "large" pits are formed as readily early in the test as later. These facts are consistent with the assumption that the pits, at least in this
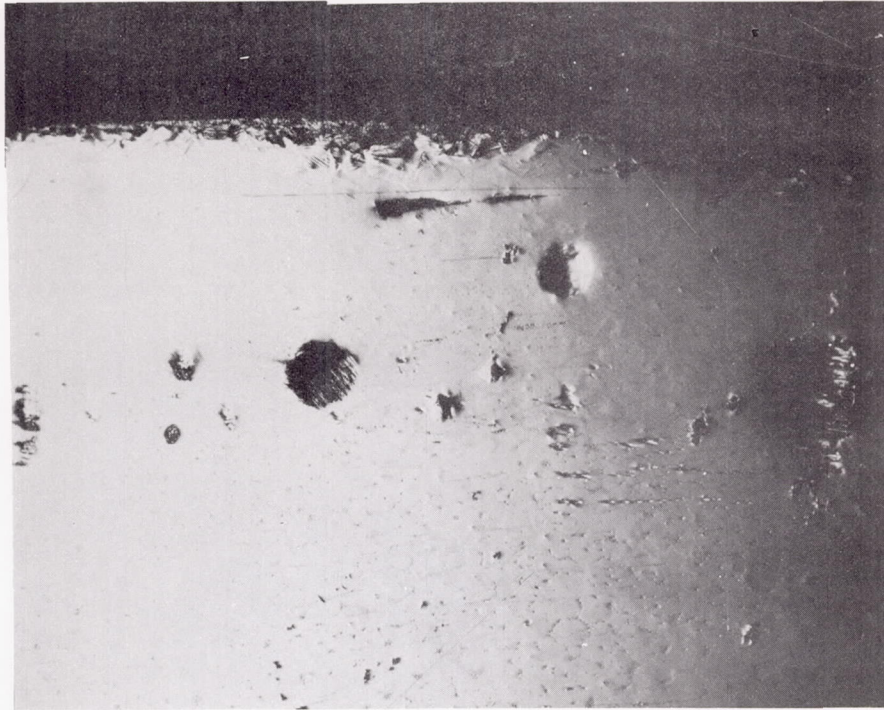
(a)
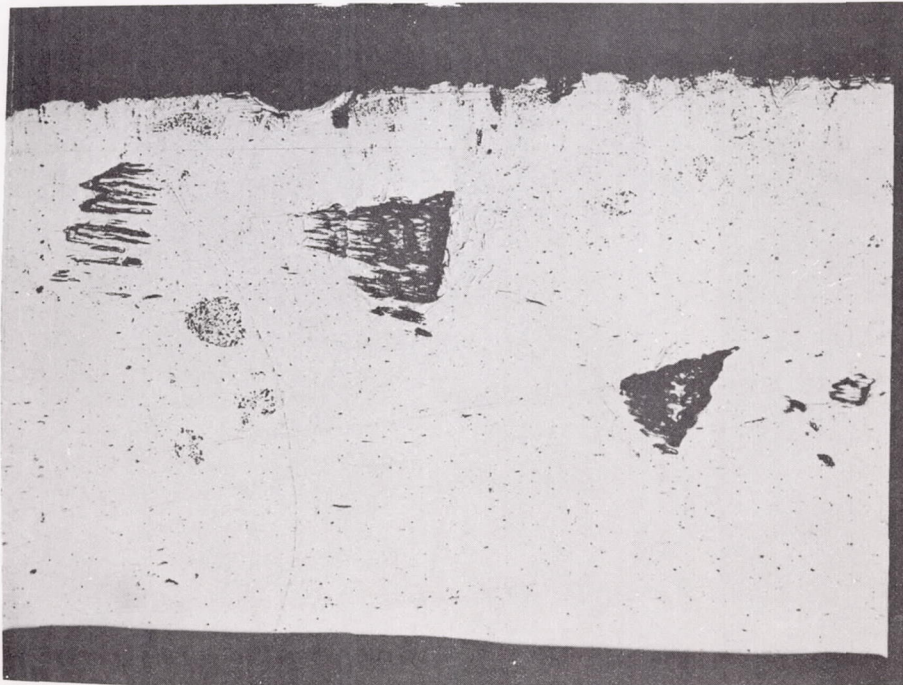
(b)

Fig. 9 Development of cavitation damage on type 302 stain-
less steel, for standard cavitation condition with
water. (Specimen 3-5; location (a) after 15 hours;
location (b) after 30 hours; throat velocity 64.7 ft
sec; x 100.)
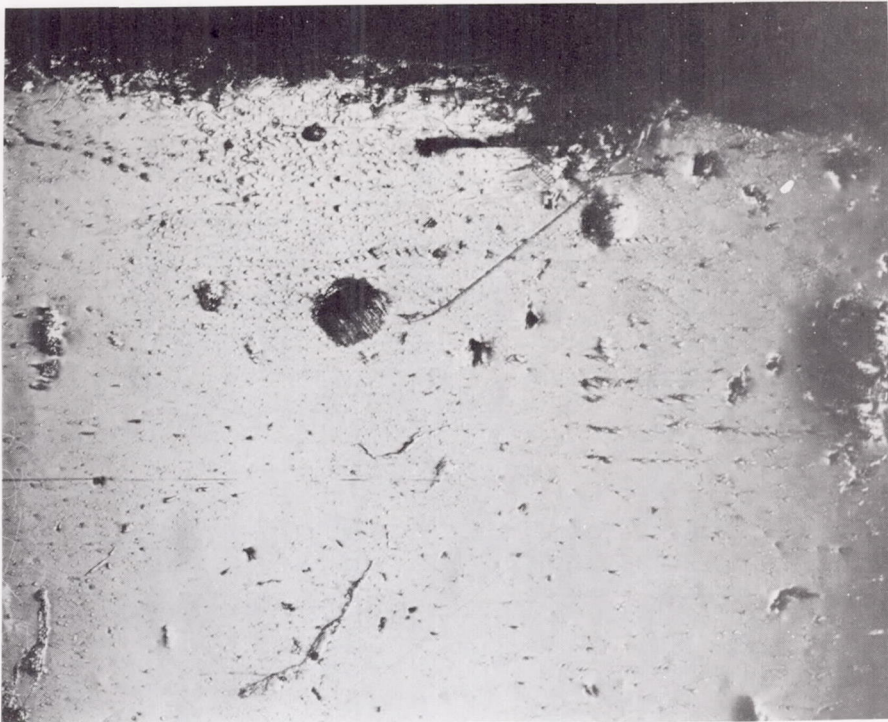
(a)
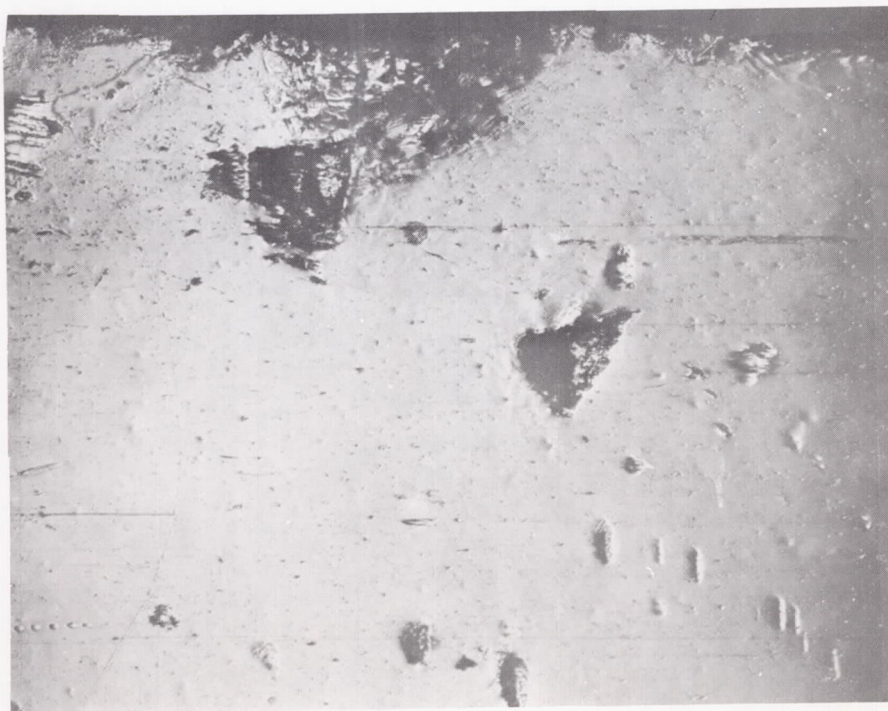
Fig. 10   Development of cavitation damage on type 302 stain-
less steel, for standard cavitation condition with
water. (Specimens 3-5; locations (a) and (b) after
150 hours, throat velocity 64.7 ft/sec; x 100.)

ROCORDER   ☐ LINEAR   ☐ TOTAL
FICORDER   ☐ ROTARY @_____ RPM —/.010"/—   PROFILE: ☐ WAVINESS   DATE____
                                                      ☐ ROUGHNESS

100 "

SET I -- Trace 3
Specimen 3 - 26

Trace recorded 2/10/61
(1 hr. wear damage)

CHART NO. 22131   MICROMETRICA

DATE_____ PART NO. 3 - 26   ☐ MICROCORDER   ☐ LINEAR
                                       ☐ PROFICORDER   ☐ ROTARY @_____ RPM

—.004/—
100

SET 2 -- TRACE 25 (Rerun)

Trace recorded 3/29/61
(11 hr. wear damage)

MICROMETRICAL MANUFACTURING COMPANY, ANN ARBOR, MICH.
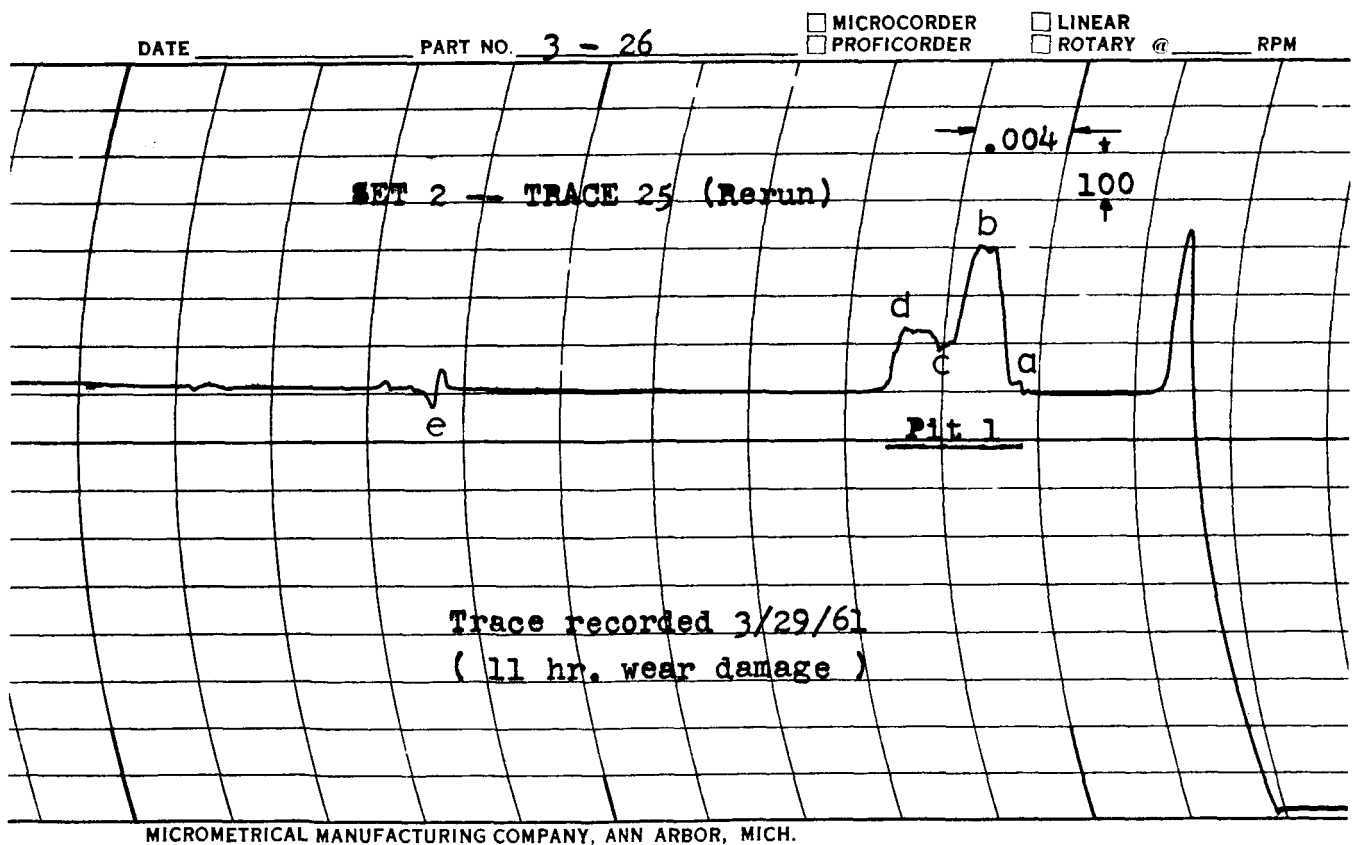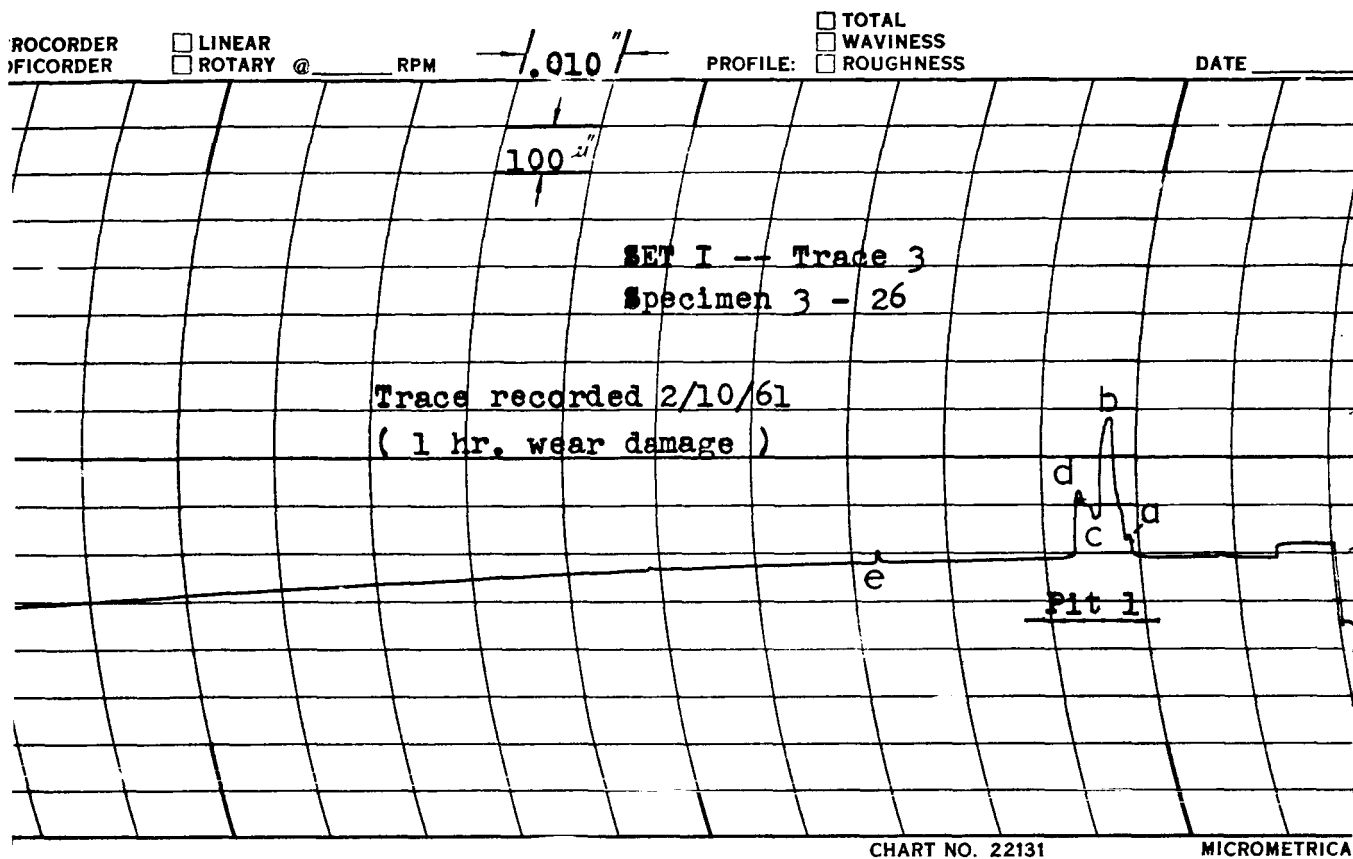
Fig. 11   Typical Proficorder traces of cavitation pit profiles
          showing the unchanged profile of the same pit after
          10 hours additional testing. (Note horizontal scale
          change from 0.010 inch/div. to 0.004 inch/div; ver-
          tical scales are 100 microinches per division.)

relatively early phase of damage, do not act as nuclei for further attack. Statistically, it is unlikely that a second large pit would overlap a previous one if their location is entirely random, since in the longest duration water runs, only about 5% of the exposed area has been affected.(1) If the location is perturbed from the random case by effects upon the material, it is likely that the bias would be such as to tend to prevent a second pitting of the same area because of the effects of local work-hardening.

Since the pits are not changed after their formation, they must have been formed in a single event, if not necessarily by a single blow. Many of the pits are virtually symmetrical craters. It is inconceivable to the writer that these could have been formed in other than a single blow because of their symmetry. However, those of irregular shape could be either the result of a single-blow or the cumulative effect of many weaker blows (fatigue failure). In any case the actual material removal must have occurred as a single event, or pits would necessarily continue to grow as exposure time is increased.

The above remarks are further corroborated by the results of the irradiated specimen run where the size distribution of the cavitation damage particles was actually measured (4) (Fig. 12). It was found that about 50% of the removed mass would not pass a filter of about 2 mil pore size. Numerically, of course, the great majority of particles are then less than 2 mil, but a substantial number are greater.[3] This roughly

---

[3] The largest single-event pits observed in the water tests are of the order of 10 mils.
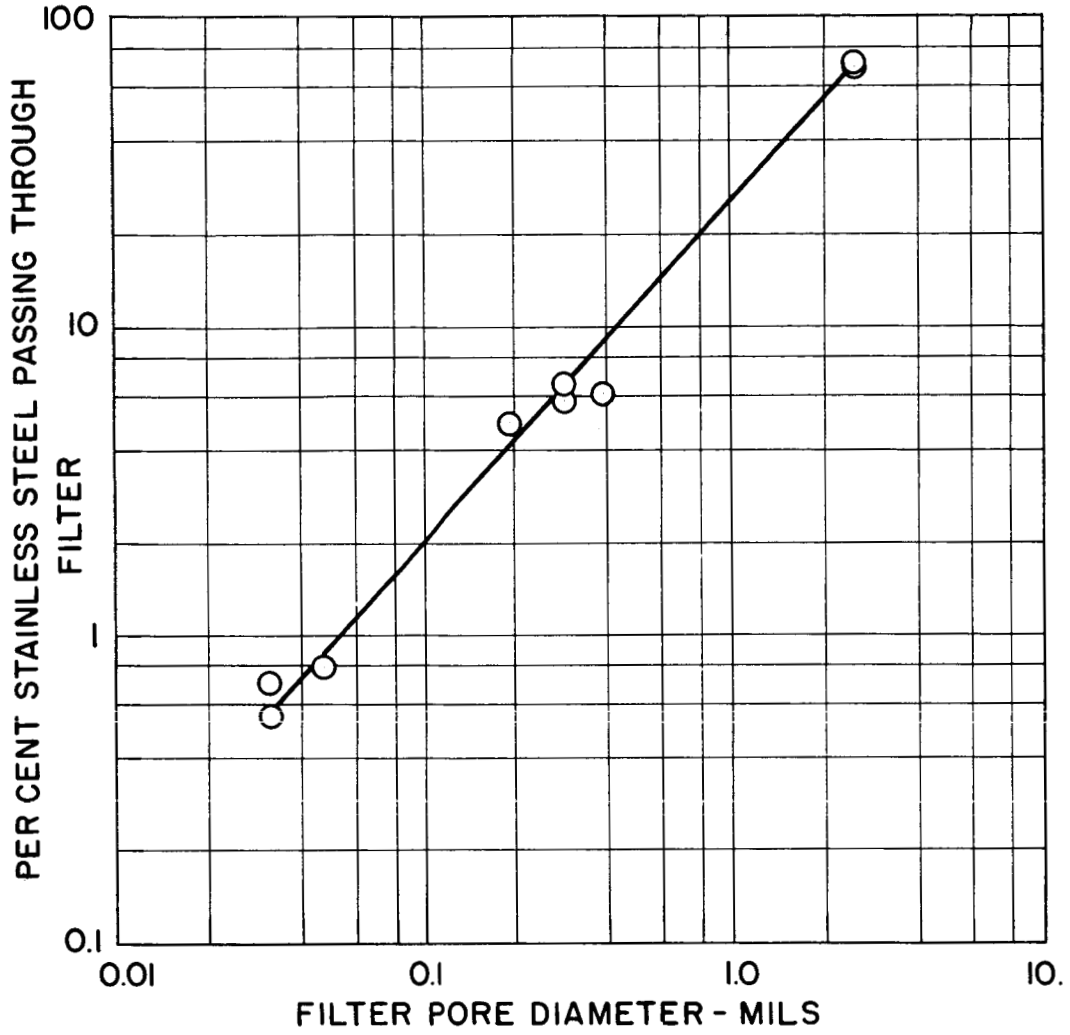
Fig. 12 Percentage, by weight, of radioactive stainless steel
         cavitation particles which pass through filter vs.
         filter pore diameter.

corresponds to the visual observations of pit size distribution.

C. Types of Pits

As mentioned briefly before, the pits are either approximately symmetrical craters, or are characterized by an entirely irregular contour. (Figures 8, 9, and 10) The proficorder traces (3) have shown that in all cases examined the diameter to depth ratio is large (order of 20). Hence the pits of irregular contour have been called slabs. It is postulated that their shape is a function of the irregularities of the surface structure (a test with an etched specimen showed, for example, that in some cases the pit outlines followed the grain boundaries) rather than of the fluid-dynamic parameters. A plausible mechanism for their formation is that the fatiguing of the underlying material results in the loosening of a small slab which is "peeled off" in the downstream direction by the stream velocity. This mechanism was suggested by Boetcher who included in his paper (5) a picture of such a slab, apparently ready to leave the surface. This mechanism has been somewhat corroborated in the present investigation by the following:

i) In about 90% of the pits examined with the proficorder (3) (no true crater has been so examined to the present) there is a ridge of material on the downstream edge of the pit only. This suggests the peeling away of a slab in the downstream direction.

ii) Slip lines have been photographed below pits in the present investigation (1) (Fig. 13) as well as in previous investigations (5 and 6 for example), indicating the presence of large mechanical stresses. These have also been indicated

-21-
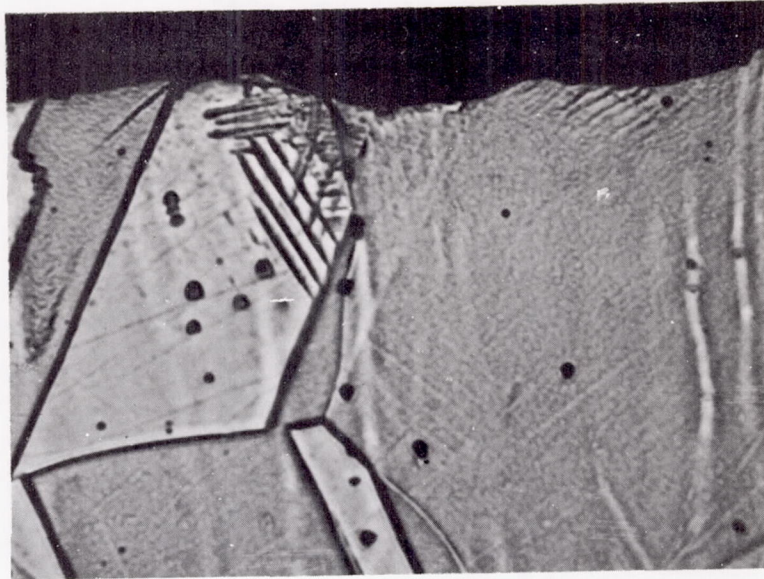
Fig. 13 Typical section through irregularly shaped pit in
stainless steel, showing slip lines. (X2000, oil
immersion, slightly oblique illumination.)

elsewhere by X-ray diffraction techniques (7) and by the use of photoelastic material (8).

In a limited number of cases in the present investigation, a very detailed pit tabulation has been made to discover the proportion of pits of the two types and their locations as a function of the various applicable parameters. The results of one such tabulation are presented in Table I. It is noted generally that the craters represent only 10% to 20% of the total pits in these water tests with no definite trends evident with the various test parameters. Since pits of this type are presumably formed in a single very intense blow, it seems likely that this proportion may increase for combinations involving denser fluids, more intense cavitation, or weaker materials. The tabulations have not as yet proceeded far enough to draw any conclusions on these matters.

D. Pit Size Distribution

Further reference to Table I indicates that the number of pits in a given size range is always substantially increased as the size under consideration is decreased. For example, there are hundreds of pits in the range 0.4 to 1.0 mils, whereas there are well less than 100 in either of the larger categories (5 to 10 and 2.5 to 5 mils, respectively). The large number of pits in the relatively uncountable smaller ranges does not introduce large errors in the volume loss calculation since the pit volume is proportional to the diameter cubed, and even the disproportionate number of pits in the smallest category has only a relatively negligible influence on the volume loss.

-23-

TABLE I

PIT COUNT TABULATIONS*

Tabulation A
Pit Count and Various Sizes

		Pit Size (mils)							
		VVL		VL		L		S	
		(10 > D > 5)		(5 > D > 2-1/2)		(2-1/2 > D > 1)		(1 > D > .4)	
		% Cir.	Total	% Cir.	Total	% Cir.	Total	% Cir.	Total
Sample No. 4-3	Polished Surface	10.0	10	23.4	17	17.33	75	12.5	400
Sample Position.......Front	Numbered Side	21.75	23	18.7	48	16.05	81	15.1	325
Standard Cavitation	Opposite Side	18.75	16	21.1	19	14.55	55	4.9	465
Throat Velocity.......64.5fps	Subtotal (2 sides)	20.5	39	19.4	67	15.45	136	9.1	790
Duration of Run.......150 hrs.	Total All Surfaces	18.4	49	21.4	84	16.1	211	10.3	1190
Sample No. 5-3	Polished Surface	15.4	13	22.2	18	25.4	110	25.8	480
Sample Position.......Back	Numbered Side	11.1	9	21.1	19	15.9	63	16.3	320
Standard Cavitation	Opposite Side	6.3	32	7.2	14	10.2	49	12.9	350
Throat Velocity.......64.5fps	Subtotal (2 sides)	7.4	41	15.2	33	13.4	112	14.5	670
Duration of Run.......150 hrs.	Total All Surfaces	9.3	54	17.7	51	19.4	222	19.2	1150
Sample No. 18-3	Polished Surface	0	11	4.5	23	6.8	74	15.0	320
Sample Position.......Front	Numbered Side	0	29	5.0	40	5.9	51	13.5	200
Cavitation to Nose	Opposite Side	0	13	9.1	11	9.1	33	12.3	130
Throat Velocity.......64.5fps	Subtotal (2 sides)	0	42	5.9	51	7.2	84	13.1	330
Duration of Run.......50 hrs.	Total All Surfaces	0	53	5.4	74	7.0	158	14.0	650
Sample No. 19-3	Polished Surface	9.1	33	17.2	64	15.0	100	10.2	365
Sample Position.......Back	Numbered Side	5.3	19	0	14	9.3	43	18.7	150
Cavitation to Nose	Opposite Side	11.1	9	0	16	7.7	26	8.6	105
Throat Velocity.......64.5fps	Subtotal (2 sides)	7.1	28	0	30	8.7	69	14.5	255
Duration of Run.......50 hrs.	Total All Surfaces	8.2	61	11.7	94	12.4	169	11.9	620
TOTAL ALL 4 SAMPLES		8.75	217	13.9	303	14.3	760	14.1	3610

Tabulation B
Pitting Intensity

					Total pits/in.^{2} - hr.							
					VVL		VL		L		S	
					(10 > D > 5)		(5 > D > 2.5)		(2.5 > D > 1)		(1 > D > .4)	
No.	Pos.	Cav. Condition	Vel.	Duration	Pol.	Side	Pol.	Side	Pol.	Side	Pol.	Side
4-3	Front	Standard	64.5fps	150 hrs.	1.79	0.87	3.05	1.49	13.44	3.04	71.7	19.6
5-3	Back	Standard	64.5fps	150 hrs.	2.33	0.915	3.22	0.74	19.7	2.50	86.0	14.9
18-3	Front	Cav. to Nose	64.5fps	50 hrs.	5.91	2.81	12.38	3.41	39.8	5.62	172.0	22.1
19-3	Back	Cav. to Nose	64.5fps	50 hrs.	17.75	1.87	34.4	2.01	53.8	4.62	196.0	17.1

Tabulation C

Summary

		VVL		VL		L		S	
		% Cir.	Total	% Cir.	Total	% Cir.	Total	% Cir.	Total
4-3	Total All Surfaces	18.40	49	21.40	84	16.10	211	10.26	1190
5-3	Total All Surfaces	9.26	54	17.65	51	19.4	222	19.2	1150
4-3 & 5-3	Total All Surfaces	13.6	103	20.0	135	17.8	433	14.67	2340
18-3	Total All Surfaces	0	53	5.4	74	6.96	158	14.0	650
19-3	Total All Surfaces	8.2	61	11.7	94	12.4	169	11.9	620
18-3 & 19-3	Total All Surfaces	4.39	114	8.94	108	9.8	327	13.0	1270
4-3 & 5-3 + 18-3 & 19-3	Total	8.75	217	13.87	303	14.34	760	14.07	3610

* Memo, L. Barinka, Nov., 1961.

It appears that pits become more and more numerous as the size category is reduced without limit below the 0.4 mil limit mentioned above. However, this is not important from the viewpoint of the volume loss calculation.

E.   **Test Material Effects**

The tests reported herein mainly involve water, at approximately ambient temperature and at close to saturation air content, as the working fluid. In a few cases mercury has been used. The test materials have been:

   i)   Stainless Steel (type 302 annealed)

   ii)   1010 Carbon Steel (annealed)

   iii)   Aluminum: a) Type 1100-0 (annealed, and b) Type 6061-T6(61-ST-6 , age-hardened)

   iv)   Plexiglas (polymethyl methacrylate)

Mechanical properties of the tested materials are listed in Table II.

On all these materials the general appearance of the pitting is similar. There are, however, significant differences between rates of pitting. Also, in the case of the carbon steel, there is significant corrosion in addition to the mechanical pitting. The damage rates for the stainless steel and carbon steel are of the same order of magnitude, with the volume loss of the carbon steel being about twice that of the stainless, prior to that period where corrosion becomes very significant (about 20 hours). In mercury the ratio is of the order of 4 at 20 hours but only 5/3 at 100 hours, based on two specimens of each material.

TABLE II

TYPICAL MECHANICAL PROPERTIES OF MATERIALS TESTED

Material	Condition	Tensile Strength psi	0.2% Yield Strength psi	% Elong. in 2 in.	% Reduction in Area	Hardness		Bending Fatigue Strength psi	Elastic Modulus
						Measured Rockwell B	BHN		
Stainless Steel Type 302	Annealed	98,000	37,000	55	65	76	140*	35,000 @ 10^7 cycles	28 x 10^6
1010 Carbon Steel	Annealed	50,000	30,000	40	71	48	85*	25,000 @ 10^7 cycles	28 x 10^6
Aluminum 1100-O(2S0)	Annealed	13,000	5,000	35	-	-	23**	5,500 @ 10^7 cycles	10 x 10^6
Aluminum 6061-T6(61-ST6)	Age Hardened	45,000	40,000	12	-	57	90*	13,500 @ 10^7 cycles	10 x 10^6
Plexiglass	-	10,445*	-	2-7	-	-	M90-M100 Rockwell**	-	0.4 x 10^6*

* Measured value or converted from measured value

** Typical value

The damage rate for the age-hardened aluminum is enormous compared to that of the steels. In fact the volume loss from the aluminum in a five-minute test is of the order of 1.5 times that of the carbon steel for an hour test under the same flow conditions, although, as shown in Table II, the hardnesses and strengths are roughly the same. No explanation for these somewhat surprising results is available at present. No quantitative test of the soft aluminum has been made, although it was noted generally that its pitting rate was many times that of the age-hardened aluminum.

The plexiglas was surprising in that its resistence to damage in the water tests was very high, superior even to the steels. Although no quantitative tests were made with plexiglas in water, it was noted that virtually no visible pitting occurred on the walls of the plexiglas venturi after hundreds of hours of exposure, and that a plexiglas damage specimen, in a relatively short test, showed considerably less pitting than the stainless steel under the same conditions. It was felt that this relative immunity to cavitation damage probably resulted from the low elastic modulus (about 1/70 that of steel, Table II), combined with relatively high strength (about 1/5 of carbon steel), in that relatively very large deflections would be required to cause the material strength to be exceeded. Since the high-pressures generated by collapsing bubbles are extremely local in nature, such deflections might remove the material from the critical area. A similar argument has been applied previously to explain the relative

immunity of surfaces coated with rubber or other elastomeric materials (9, for example). However, the volume loss for plexiglas tested in mercury was found to be greater than that of carbon steel by a factor of about 10. The reason for the inconsistency of the results between water and mercury is not at present known.

F. Fluid Effects

Only two fluids have been involved so far: approximately ambient temperature water, and mercury. Whereas an initial set of water runs has been completed, the initial mercury tests are still in progress. However, certain significant trends are evident.

i) The wear rate with mercury is apparently several orders of magnitude greater than that with water. At present there is some uncertainty regarding the exact ratio for any given test since the weight losses with mercury are large enough for direct measurement with good precision, while those with water were not, so that the somewhat tenuous calculations based on pit tabulations were necessary. Although the irradiated specimen test with water is a form of direct measurement, there are various possibilities of significant error which cannot be evaluated until additional tests are made. Hence a precise comparison is not possible until the test procedures have been developed to better precision, and the pit count data obtained with mercury have been reduced and compared with the direct weight losses. However, a "best guess" damage ratio between mercury and water damage rates at approximately

the same fluid-dynamic conditions is the order of 90. Incidentally, because of its ability to produce damage rapidly, mercury is a very useful cavitation damage test fluid.

ii) The type of pitting encountered with mercury and water is generally similar. However, the mercury test series and the examination of the data produced are not sufficiently advanced to allow more detailed conclusions.

G.   Flow Parameter Effects

The flow parameters which have been varied significantly in the present tests are cavitation condition and throat velocity. Their effects are discussed below.

1.   Cavitation Condition[4]

Independent of throat velocity, the cavitation condition ("degree of cavitation") can be varied from "zero cavitation" through initiation to fully-developed conditions (First, and Second Mark), wherein the region of visible cavitation terminates considerably downstream of the trailing edge of the test specimen. From the viewpoint of cavitation damage, the significant difference between these conditions is the pressure existing in the vicinity of the test specimen. As the degree of cavitation is adjusted toward the more developed conditions, the pressures in the vicinity of the test specimen decrease, eventually reaching values close to the vapor pressure. Such a direction of adjustment results in two diverse trends:

i) The number of bubbles in the vicinity of the test

---

[4]Defined in appendix.

specimen increases as the degree of cavitation is
increased.

ii) The driving pressure differential for bubble collapse
decreases. (Typical axial pressure profiles are shown
in Fig. 14 for all the cavitation conditions.)

When the degree of cavitation for the water tests is
reduced to "visual initiation", for example, there is no cavi-
tation visible on the test specimen. However, small, local
cavitation regions, induced by the test specimen itself must
exist since the damage in this condition is significant. Thus
it appears that a small number of highly energetic bubble
collapses can be more harmful than enormously greater numbers
of less energetic bubbles. This trend is further evidenced by
the fact that very little damage is sustained when the cavita-
tion region entirely envelopes the test specimen. On the other
hand, "sonic initiation", wherein no cavitation is visible, also
produces very little damage. (Even though a large pressure
differential is available in the vicinity of the test specimens
for bubble collapse, too few bubbles for significant damage
penetrate far enough.) Finally, if the throat pressure is
raised considerably above that corresponding to sonic initia-
tion the pitting rate is reduced another order of magnitude
(apparently pure erosion from single-phase flow also produces
pitting of similar appearance, but in considerably reduced
quantity). These results are illustrated graphically for water
in Fig. 15.

Although not yet entirely evaluated, the results with
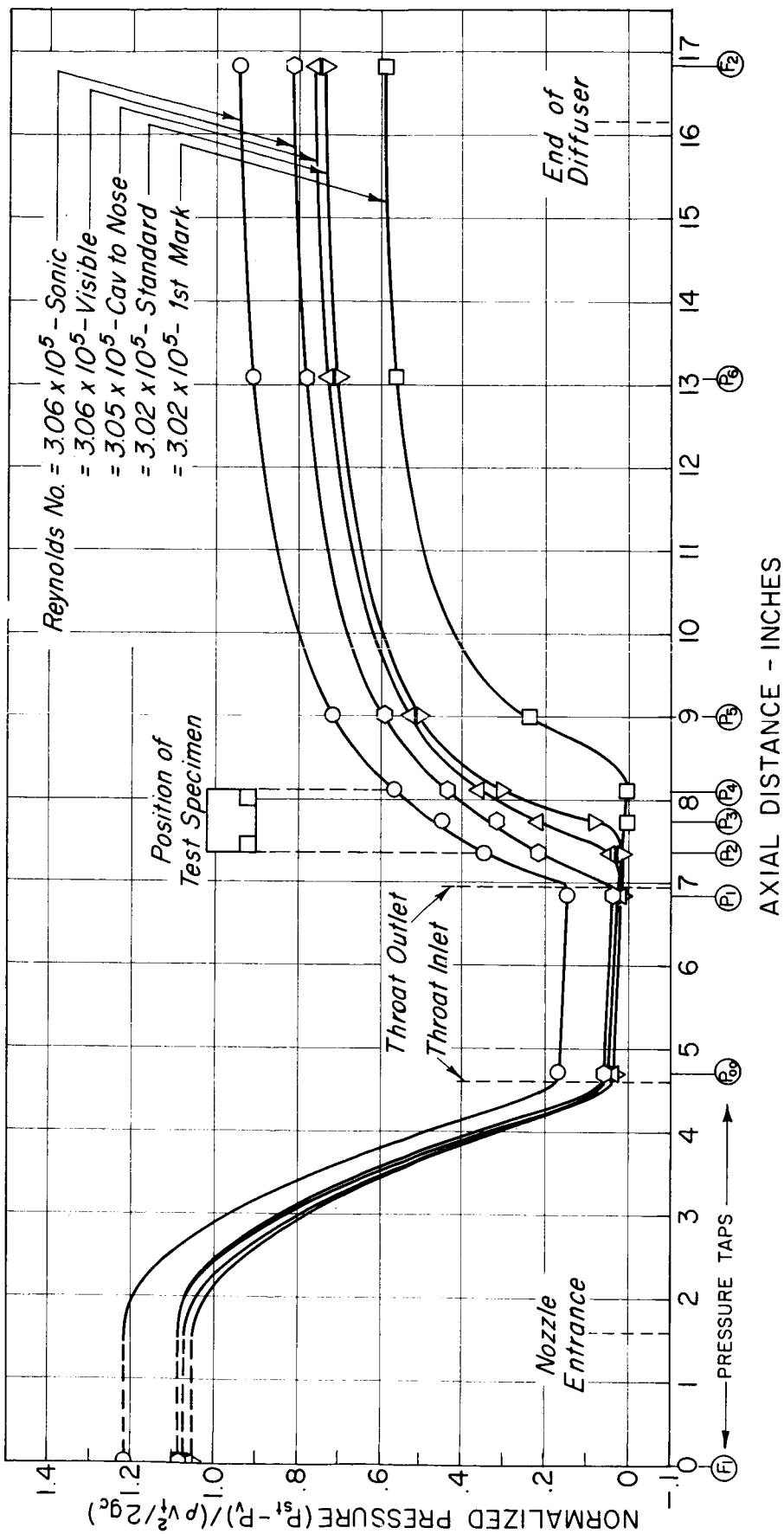mercury appear different in that the bubbles do not penetrate

Fig. 14 Normalized axial pressure profiles for several cavi-
tation conditions with water ($\frac{1}{2}$ inch venturi test
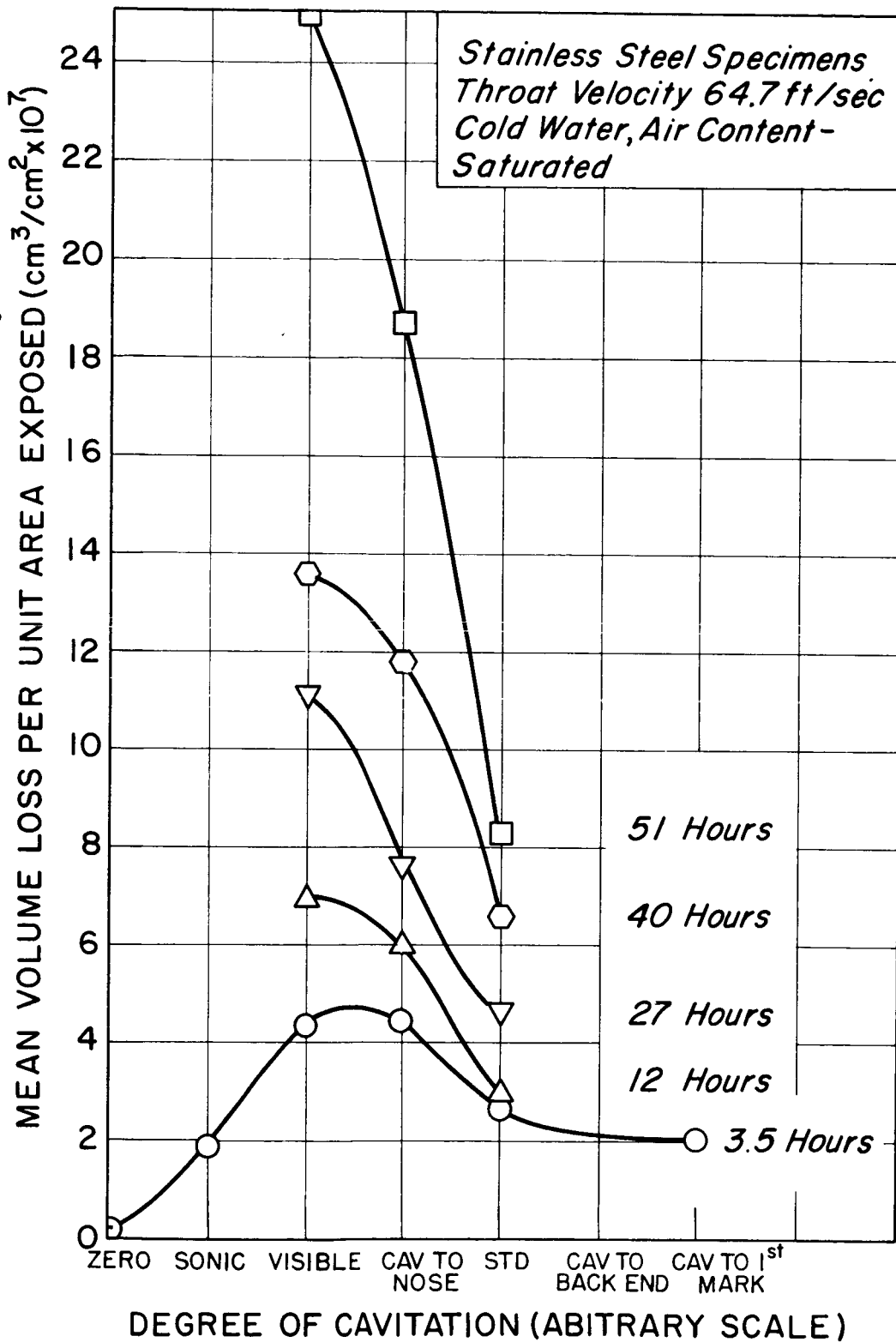section No. II).

Fig. 15 Mean volume loss per unit area of specimen exposed to
fluid vs. degree of cavitation, for pairs of stain-
less steel specimens in water.

so far into the high pressure regions. For example, sonic and visible initiations, and even cavitation to the specimen nose, produce relatively little damage, so that the maximum damage is produced by the relatively well-developed conditions of standard and first mark. These results are shown for a typical case in Fig. 16. The reason for the inconsistency in this respect between water and mercury will have to await a theoretical analysis of the applicable bubble mechanics problem, which is presently being attempted.

2. Throat Velocity

Throat velocity for either fluid has been varied over a factor of about two. The effects upon wear have not been as great for any of the materials as expected judging from the observations of previous investigators (for example, the approximate 6th power effect[5] observed by Knapp (10) and others (11, 12, 13)). However, it is not obvious to the writer that in an arrangement such as the venturi of the present tests, an increase of throat velocity should correspond to a large increase in damage, unless the pressures in the vicinity of the test specimen are also substantially increased, without a corresponding dimunition in the number of bubbles. The fulfilling of these conditions is of course a function of the degree of cavitation used. In any case the mechanism in the present flow arrangement whereby the throat velocity affects damage rate is neither clear nor simple.

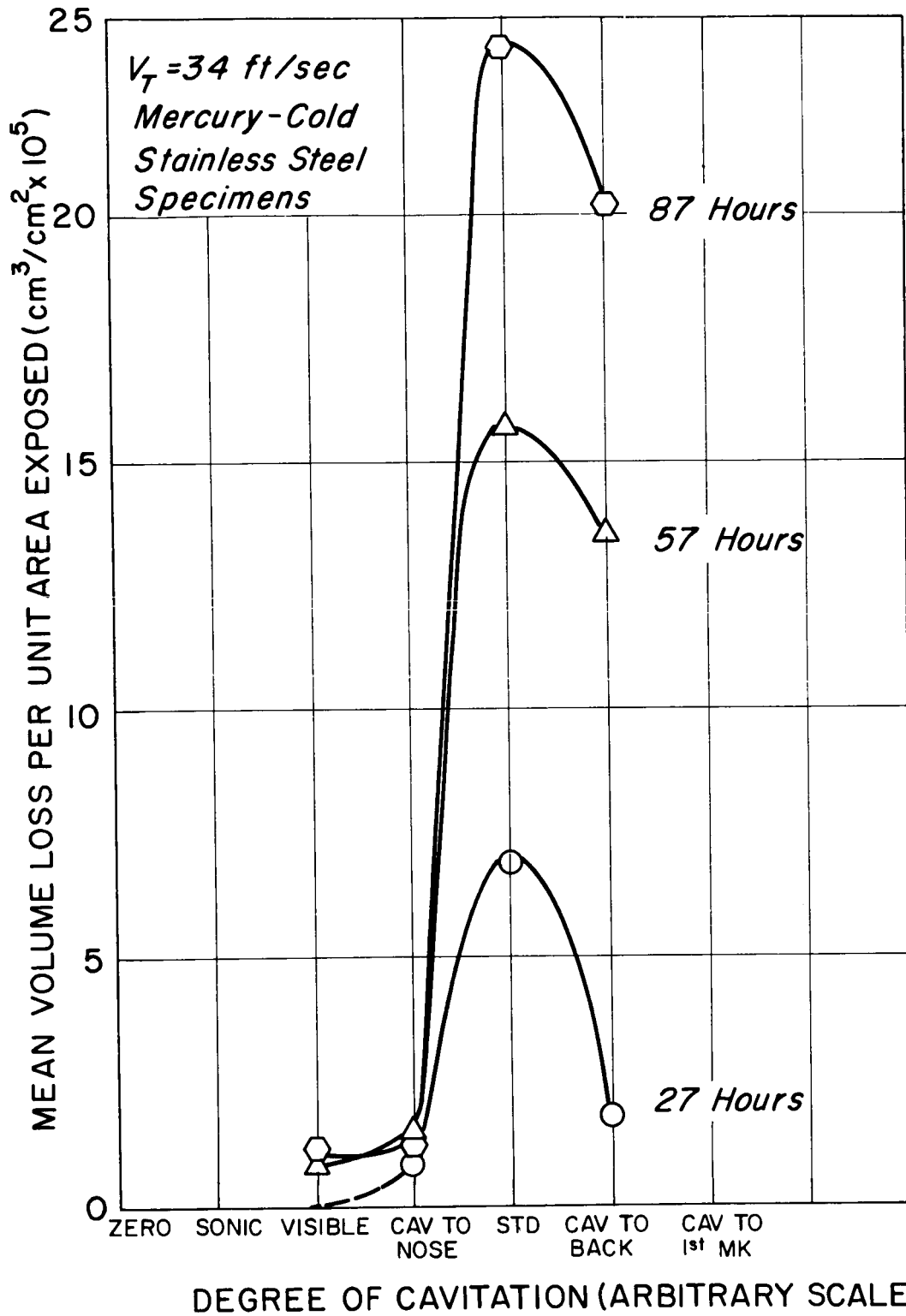
[5] Assuming Damage $\propto V^n$.

Fig. 16   Mean volume loss per unit area of specimen exposed to
fluid vs. degree of cavitation, for pairs of stain-
less steel specimens in mercury.

The available comparisons from the present tests with water show a maximum velocity-damage exponent of about 4.9 for a 12-hour test of stainless steel for standard cavitation. Other exponents obtained are:

i) 3.9 for a 3.5 hour test under the above conditions

ii) 2.4 for a 1.0 hour test of carbon steel

iii) 1.7 for a 5-minute test of age-hardened aluminum.

It is noted that all the presently available tests are for standard cavitation, wherein the pressure in the vicinity of the test specimen is relatively moderate for all velocities (Fig. 14). It may well be that greater velocity effects would be observed if a less-developed cavitation condition, with higher and more velocity-dependent test specimen pressures had been used.

The damage-exponent is plotted in Fig. 17 against test duration. It is noted that a very smooth curve results even though the materials used for each duration (except the two longer) are different. Whether or not this result is purely coincidental is not presently known. Further corroboration from additional tests must be awaited.

The preliminary data from the mercury tests do not indicate even as great a velocity effect as that found with water. However, more precise conclusions are not yet possible.

There is no indication in the present tests of the exist-ence of a threshold velocity as sometimes reported in the past (11, 13, 14). However, the velocities have not been carried low enough so that definite statements in this regard can be made.
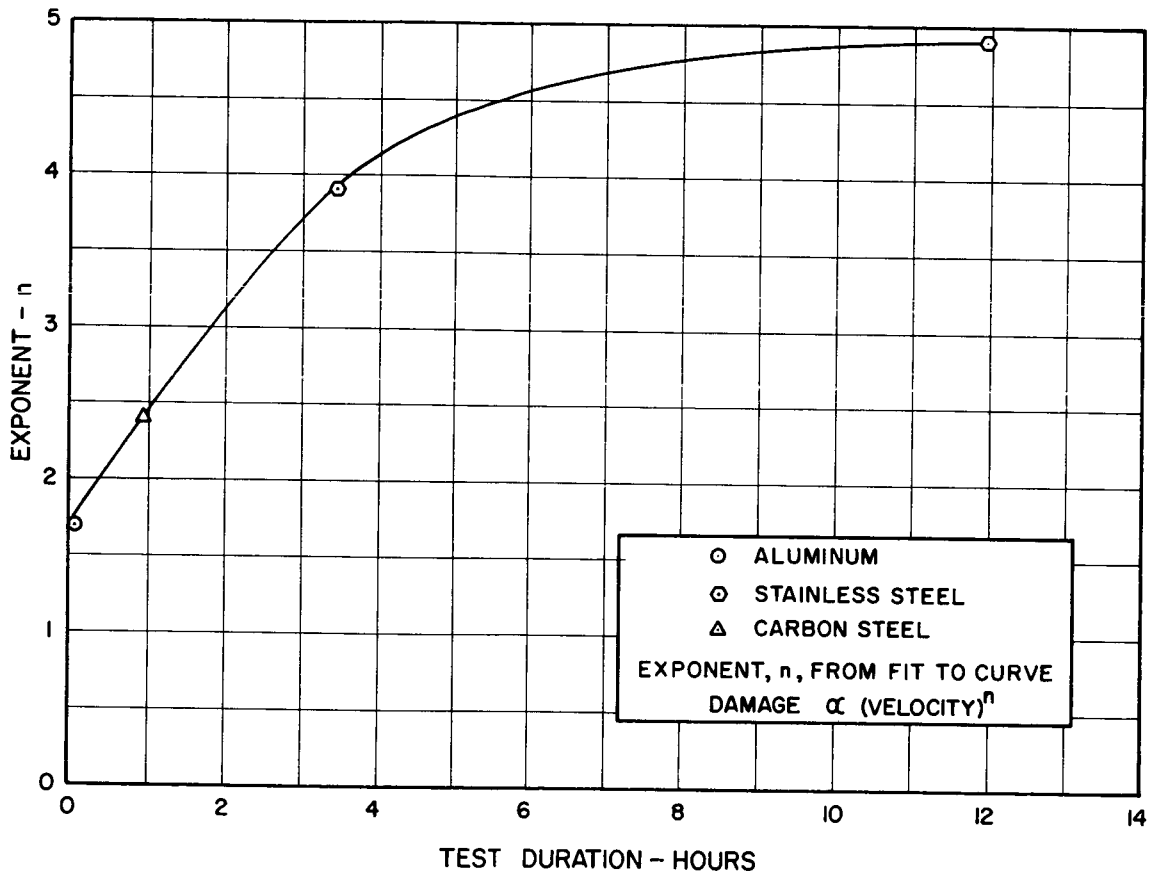
Fig. 17 Value of exponent, n, vs. test duration, for several specimen materials in water.

IV Discussion of Results

It is possible to obtain fairly comprehensive results in an investigation similar to that described herein by testing a variety of materials with different fluids, and under different fluid-dynamic conditions. However, some unifying hypothesis or correlating method is required to bring order out of the otherwise somewhat chaotic conditions which result. A bubble energy quantum approach was previously suggested by the writer for this purpose. (1, 15)[5]

A hypothesized bubble energy quantum spectrum is shown in Fig. 18 in a shape suggested by the data and the existing knowledge of bubble dynamics. The ordinate, $n(E)$, is the number of bubbles from those "in the vicinity" of the damage specimen which deliver, upon their collapse, an energy quantum, E, to the surface of the specimen. The abscissa is E, the energy quantum. The shape of any of the individual curves is a function of the cavitation condition, which is thus the parameter distinguishing the different curves. Generally, the hypothesized curves show a maximum number of bubbles of relatively small energy, and increasingly smaller numbers of more energetic bubbles. The curve shape could be quantitatively investigated by using high-speed motion pictures to delineate the bubble-size spectrum, and by using bubble-dynamics studies to compute the energy quantum delivered to the surface per bubble, under the known external pressure conditions (corresponding to the cavitation condition and the throat velocity).

As the cavitation condition becomes less fully-developed,

---

[5]A model which is somewhat similar has also been previously proposed by Rao and Thiruvengadam (16). However, the conceptions were independent.
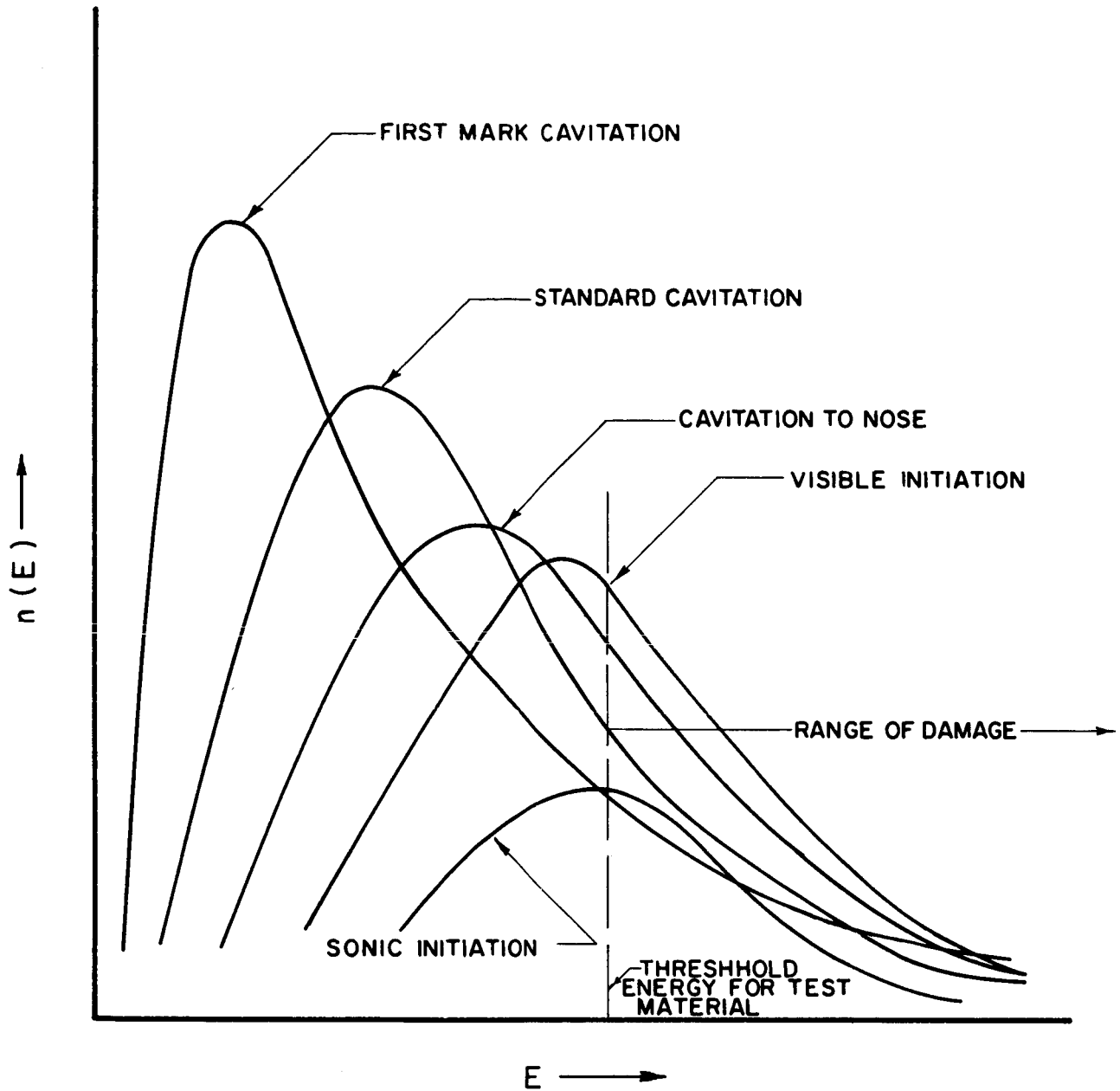
Fig. 18   Hypothesized bubble energy spectra for various
          cavitation conditions at a constant velocity, for a
          given material. Presumably, curves at higher velocity
          are generally similar, but at higher n(E) and E. The
          quantity n(E) = number of bubbles from those "in
          vicinity" of damage specimen which deliver an energy
          quantum E to the surface of the specimen, and E =
          energy delivered by an individual bubble to the
          surface of the specimen.

the total number of bubbles decreases, but the number at relatively high energy increases, at least until the cavitation condition is reduced to a minimum. This is illustrated by the curves (Fig. 18), the arrangement of which was guided by the water damage results, showing a maximum of damage for cavitation to nose and visible initiation, and a minimum for sonic initiation and first mark (the condition for zero cavitation would, of course, correspond to the abscissa).

It is assumed that at least a minimum energy quantum, E, is required to produce any damage. (The surface stress must at least exceed the endurance limit.) Hence, a threshold value for E is shown, which is obviously a function of the test material. (For harder and/or stronger materials this threshold would move to the right.) A second threshold, further to the right, is shown for single-blow damage (corresponding to the crater-type pits). The total amount of damage which occurs in the form of slabs or craters respectively, is proportional to the integral under the applicable curve to the right of the applicable threshold.

While a set of curves as described above would only be applicable to a given fluid[6] and flow geometry, i.e., for example, a venturi of a given design, this approach appears to the writer to present a potentially extremely useful method for correlating cavitation damage results. This general type of behavior is also evidenced by tests with magnetostriction devices reported by Nowotny (17) in which the fluid temperature is varied over the range between solidification temperature and

---

[6]For example, similar curves for mercury (rather than water) would probably be displaced to the right, i.e., to the higher energy range.

boiling temperature at a constant pressure. It is found that
the damage reaches a maximum at some temperature well below the
boiling temperature (as low as 50° C for atmospheric pressure
in some of Nowotny's work). Presumably, at temperatures near
the boiling temperature there are very many bubbles but the
collapse energy is small, so that the damage is small. At
lower temperatures, there are fewer but more energetic bubbles
with resultant increased damage. As the temperature is reduced
still further, the energy of the individual bubbles continues
to increase, but the number of bubbles becomes extremely small,
so that the resultant damage decreases.

V Conclusions

A fairly comprehensive set of cavitation damage data
obtained in a flowing system (venturi) over a relatively wide
range of applicable parameters has been presented. Detailed
conclusions regarding the effects of the variation of the
different parameters are pointed out and discussed in the body
of the paper. Finally, a correlating model to illustrate the
effects of these different parameters is suggested.

It is apparent from all of the above that much work yet
remains to be accomplished in this field before it will be
possible to predict with any degree of certainty the cavitation
damage to be sustained in various fluid flow components under
applicable operating conditions. However, in the writer's
opinion, this does not appear to be an impossible objective,
and, in fact, considerable progress toward attaining it is
being made.

1. F. G. Hammitt, et al., "Cavitation Damage Tests with Water in a Cavitating Venturi", ORA Technical Report 03424-4-T, University of Michigan, March, 1962.

2. F. G. Hammitt, et al., "Observations and Measurements of Flow in a Cavitating Venturi", ORA Technical Report 03424-5-T, University of Michigan, May, 1962.

3. V. F. Cramer and F. G. Hammitt, "Cavitation Pit Diameter-Depth Observation for Stainless Steel in Water", Internal Report No. 9, ORA Project 03424, University of Michigan.

4. W. J. Walsh and F. G. Hammitt, "Cavitation and Erosion Damage Measurements with Radioisotopes", Trans. ANS, Vol. 4, No. 2, Nov., 1961, p.247; to be published, Nucl. Sci. and Eng.

5. H. N. Boetcher, "Failure of Metals Due to Cavitation Under Experimental Conditions", Trans. ASME, Vol. 58, 1936, pp. 355-360.

6. J. M. Mousson, "Pitting Resistance of Metals Under Cavitation Conditions", Trans. ASME, Vol. 59, 1937, pp. 399-408.

7. M. S. Plesset and A. T. Ellis, "On the Mechanism of Cavitation Damage," Trans. ASME, Vol. 77, No. 7, Oct. 1955., pp. 1055-1064.

8. A. T. Ellis, "Production of Accelerated Cavitation Damage by Acoustic Field in Cylindrical Cavity", Acoustical Society of America Journal, Vol. 27, No. 5, Sept., 1955, pp. 913-921.

9. J. Z. Lichtman, "Possible Contributions of Reentrant Flow to Cavitation Erosion", ASME Paper No. 62-HYD-3, 1962.

10. R. T. Knapp, "Recent Investigations of the Mechanics of Cavitation and Cavitation Damage", Trans. ASME, Vol. 77, 1955, pp. 1045-1054.

11. J. M. Hobbs, "Problems of Predicting Cavitation Erosion From Accelerated Tests", ASME Paper No. 61-HYD-19, 1961.

12. S. L. Kerr and K. Rosenberg, "An Index of Cavitation Erosion by Means of Radioisotopes", Trans. ASME, Vol. 80, 1958, pp. 1308-1314.

13. J. Z. Lichtman, D. H. Kallas, C. K. Chatten, "Study of Damaging Effects of Cavitation Erosion to Ships' Underwater Structures", Trans. ASME, Vol. 80, 1958, pp. 1325-1339.

14. D. J. Godfrey, "Cavitation Damage--A Review of Present Knowledge", Chemistry and Industry, June 6, 1959, pp. 686-691.

15. F. G. Hammitt, "Proposed Model for Cavitation Pitting and Related Thoughts", Memo to File, University of Michigan ORA Project 03424, October 6, 1961.

16. Rao, N.S., and Thiruvengadam, A., J. Hyd. Div., Proc. Am. Soc. Civ. Eng., September 1961, pp. 37-62.

17. H. Nowotny, Werkstoffzerstorung durch Kavitation, V. D. I. Verlag Gimbh, Bertin, NW 7, 1942, English Translation published by Edwards Brothers, Ann Arbor, Michigan.

Specification of Cavitation Conditions

The cavitation condition for all tests is defined in terms of "degree of cavitation", referring (except for initiation) to the extent of the cavitating region.

i) Sonic Initiation - First sonic manifestation beyond that of single phase flow. This was detected either by ear or electronically using a piezoelectric crystal. The results of these two methods were approximately the same. In all cases, sonic initiation occurred at a higher throat pressure than visible initiation.

ii) Visible Initiation - First appearance of a more or less complete ring of cavitation. This always appears first at the throat exit.

iii) Cavitation to Nose - The approximate location of the termination of the cavitation region is at the upstream nose of the test specimen.

iv) Standard - The approximate location of the termination of the cavitation region is at the center of the test specimen.

v) First Mark - The approximate location of the termination of the cavitation region is about 1 3/4 inches from the throat outlet.

vi) Second Mark - Same as first mark, but at $3\frac{1}{2}$ inches.

vii) Cavitation to back end - the approximate location of
the termination of the cavitation region is at the
downstream end of the test specimen.

The location of these termination points is shown in
Fig. 2. Although the termination is not sharp, the cavitation
conditions can be quite precisely reproduced.